

High-pressure behavior of quasi-one-dimensional 2H-CsCdBr₃

J. C. Chervin

Physique des Milieux Condensés, Université Pierre et Marie Curie, 4 place Jussieu, 75252 Paris Cédex 05, France

C. Andraud, N. Tercier, and B. Blanzat

Laboratoire de Physico-Chimie des Matériaux, 1 place A. Briand, 92190 Meudon, France

E. Cazzanelli

Dipartimento di Fisica, Università degli Studi di Trento, I-38050 Povo (Trento), Italy

J. M. Besson

Physique des Milieux Condensés, Université Pierre et Marie Curie, 4 place Jussieu, 75252 Paris Cédex 05, France

(Received 19 May 1988)

Hexagonal 2H-CsCdBr₃ has a strongly anisotropic bonding scheme: ionicovaleant CdBr₆ chains are separated by cesium ions. Analysis of the Raman-active modes up to 25 GPa shows no phase transition. The behavior of the modes is similar to that of other one-dimensional crystals, although mechanical properties (compressibility) show little anisotropy. A qualitative model is proposed to evaluate the variation of interatomic distances under pressure.

INTRODUCTION

A class of ternary ABX_3 compounds have the cubic perovskite structure. Here, A is a monovalent large cation, B a divalent small cation, and X some halogen anion. Regular $(BX_6)^{4-}$ octahedra are connected by their corners. This structure can be deformed to lower symmetry via phase transitions, usually driven by decreasing temperature. This leads to large changes of dielectric properties. In any case, the tridimensional character of the bonds is maintained. Another class of compounds with the same chemical formulas have hexagonal structures with face-sharing¹ $(BX_6)^{4-}$ octahedra (Fig. 1). A trigonal distortion of the octahedra along the c axis stabilizes the structure and moves the three halogen ions closer together to screen the direct B cations interaction. However, this compensation may not be sufficient to completely stabilize the structure since several intermediate polytypes occur with different ratios of face-sharing to corner-sharing bonds. This is related to the ratio of the relevant ionic radii (Goldschmidt tolerance factor),¹⁻⁴ which can be varied either by atomic substitution or by application of high pressure. Adequate combination of high pressure and heat treatment will induce a series of phase transitions, the common sequence of polytypes being 2H-9R-4H-6H-cubic perovskite, with increasing pressure and increasing fraction of "cubic" bonds; along this sequence, the chains of face-sharing octahedra decrease in length and the number of octahedral units per chain is infinity-3-2-2-0. The last figure means absence of face-sharing bonds in the cubic perovskite. These intermediate structures have hexagonal symmetry with different primitive cells, except for 9R (D_{3d}^5 space group).

In the case of CsCdBr₃ ["infinitely" long chains (Fig. 1)], the difference between the ionicovaleant intrachain interaction^{5,6} along the crystal c axis and the purely ionic interchain bonds is expected to induce a strong anisotropy of this structure which can be regarded as quasi-one-dimensional (1D). The effects of this anisotropy of nearest-neighbor interactions have been observed on the magnetic ordering in compounds with magnetic (Fe, Co, Ni, etc.) B atoms.^{7,8} Isostructural diamagnetic compounds (CsMgBr₃; CsMgCl₃) are useful host matrices for optical and magnetic studies of transition-metal ion impurities.⁹⁻¹¹ Polytypic transformations under high pressure and temperature have been obtained in fluoride crystals, as well as in ABO_3 oxides, with the same polytypic sequence. These transitions which effectively alter the dimensionality of the crystal occur below 10 GPa and show large hysteresis;^{2,3} a combination of temperature quenching and sudden release from high pressure yields the high-temperature, high-pressure forms which are metastable at ambient, where their structure can be easily determined.

Interestingly enough, nevertheless, no high-pressure study of these structures, particularly the 1D, 2H polytype, has been carried out yet at room temperature, although high pressure is known to have large effects on low-dimensionality crystals such as molecular crystals (sulfur), 1D chainlike compounds (SbSI), or 2D layer compounds (GaS-GaSe). Among others the lattice vibrations of those crystals usually show a distinct difference under high pressure between the intramolecular (intra-chain, intralayer) modes and the intermolecular ones, the latter having relative pressure derivatives orders of magnitude larger. The first point of the present study was thus to ascertain whether the one-dimensional bonding

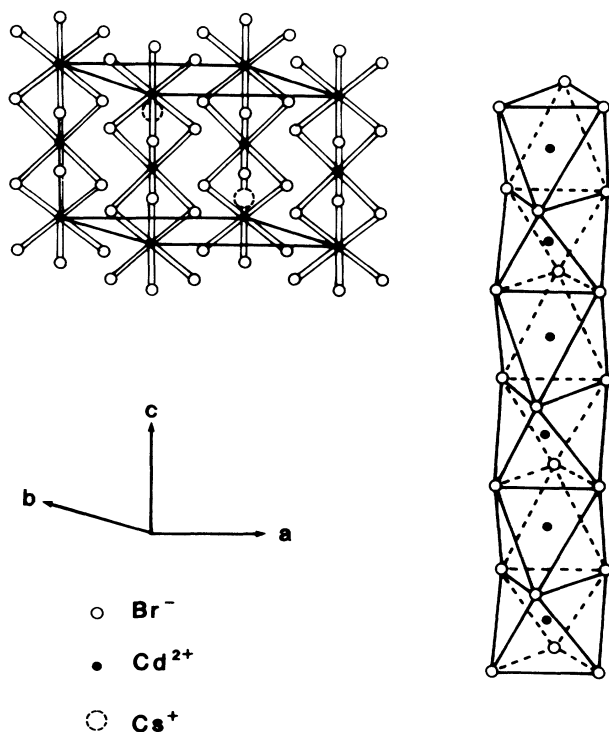


FIG. 1. Crystal structure and bonding scheme of CdCsBr₃. Left-hand side, unit cell with $a = 7.675 \text{ \AA}$, $c = 6.723 \text{ \AA}$. Cell volume, 343 \AA^3 . Right-hand side, perspective view of the octahedral CsBr₆ chains, cesium atoms not shown.

scheme of these crystals, 2H-CsCdBr₃ in this case, was indeed reflected in the high-pressure evolution of the phonon modes.

The second point of interest is the stability of this low-symmetry structure under high pressure, and the possible occurrence of polytypic transformations. It should be remembered that low-dimensionality structures, particularly 1D and 2D crystals, usually show remarkable stability under high pressure, in contrast with 3D crystals, the most classical case being graphite, which will not transform to diamond directly without application of high temperature and adequate (Ni,Co,Fe) solvents. Other cases are layered structures like GaSe or GaS (Refs. 12–14) which remain lamellar up to 20 GPa and do not transform to a 3D bonding scheme even when interlayer bonds have become stronger than intralayer ones. By contrast, a majority of 3D crystals exhibit one or several phase transitions below 10 GPa.

We therefore studied CsCdBr₃ under pressures up to 25 GPa at room temperature, measuring the shift of its Raman-active modes. We will first examine the structure of the crystal and model its evolution under pressure, then briefly describe the experimental setup and methods in Sec. II. The results will be discussed in Sec. III as regards the frequency shifts, the evidence for phase transitions, the change in Raman linewidths, and finally the evolution of Raman scattering cross sections under pressure.

I. STRUCTURE AND BONDING SCHEME

CsCdBr₃ has the $P_6/mmc (D_{6h}^4)$ space group (2H polytype) with two formula units per primitive cell. The (CdBr₆)⁴⁻ octahedra would be connected in infinitely long chains in the ideal crystal. Lattice parameters⁸ are $a = 7.675 \text{ \AA}$ and $c = 6.723 \text{ \AA}$. Because of a trigonal distortion, the distance between the Br⁻ ions in a direction perpendicular to the c axis is smaller than along the axis (3.814 and 4.019 \AA). As in other isomorphous compounds, the Cd—Br bond has appreciable covalent character, which accounts for the directionality of the bonds, along the chains. This can be inferred from the difference between the ionic radius of the Cd²⁺ ion¹⁵ and its value in this series of isomorphs.⁷ On the contrary, Cs⁺ cations may be considered as fully ionized and have pure Coulomb interaction with the chains which accept one electron per (CdBr₃)⁻ unit to preserve the chemical valency. The outer electronic shell of Cs⁺ is thus saturated and is that of xenon. It is surrounded by 12 nearest-neighbor bromine, which form a distorted rhombododecahedral cage: 6 are at the same ordinate on the c axis and 6 more at different ordinates (3 above and 3 below). The Cs-Br distance for the former group is $a/2 = 3.8375$ and 4.033 \AA for the latter. The ionic radius of Cs⁺ being only 1.60 \AA , its saturated electronic outer shell is very weakly perturbed by its dodecahedral environment at ambient pressure.

II. EXPERIMENTAL

CsCdBr₃ crystals were grown by the Bridgman method under bromine gas pressure.^{10,11} Preferential cleavage planes contain the crystal c axis and intersect each other at 120°. The impurity content has been found to be lower than 10 ppm. Comparison of the optical properties of pure CsCdBr₃ and Pb²⁺-doped samples^{10,11} shows that undoped crystals have a high degree of disorder, probably due to broken chains. Among others, this disorder increases the Raman linewidths^{16,17} and may be partly responsible for the incomplete agreement with selection rules of the observed Raman intensities: the analysis of polarized Raman spectra has thus been made difficult because of mixing between contributions with different symmetries.

Samples used for high pressure were unpolished cleaved chips with the axis in the plane of the sample, typically 100 μm across and 20 μm in average thickness. The diamond anvil cell¹⁸ was used with a 180- μm hole in a prestrained 100- μm -thick Inconel 750 gasket. Ethanol and methanol being solvents for CsCdBr₃, argon was used as a pressure transmitting medium up to 25 GPa with some low-pressure data taken in silicone oil which remains fluid up to some 5 GPa. Pressure was measured by the fluorescence lines of ruby chips (Al₂O₃: 3000 ppm Cr³⁺) using the nonlinear Bell and Mao scale,¹⁹

$$P_{\text{GPa}} = 380.8 [(\lambda/\lambda_0)^5 - 1]. \quad (1)$$

Spectral lines from a low-pressure neon lamp were used as an absolute frequency reference both for ruby luminescence and for Raman spectra. The pressure data were

collected before and after each Raman run to have control over possible pressure shifts during the scan itself. Raman spectra were excited with light from the 514.5-nm line of an Ar⁺ laser and analyzed with a T800 Coderg triple monochromator. The instrumental resolution with 300- μm slits was about 3 cm^{-1} but the wave-number precision was better than 0.2 cm^{-1} . Although the observed Raman lines are somewhat broadened by the instrumental function, this does not alter our conclusions since here we discuss only variations of linewidths with pressure.

Reproducibility of the optical alignment was checked to be within 10% between successive runs after removing and replacing the cell so that the relative Raman intensity variations we discuss later are significant within this error for a given sample, for the strongest peaks. To take into account the variations in width of individual peaks, the intensities given in Sec. III are the product of the height of the Raman peaks times the FWHM (full width at half maximum), which is close enough to the actual integral for our purpose. The intensity of each line is then expressed as the percent of the total Raman intensities of all five modes observed. Actually the total Raman signal (sum of all modes) did not significantly vary with pressure. This indicates that no pressure-induced absorption or resonant scattering occurred with the laser wavelength we used here. Results for the weakest modes are less precise since the signal had to be extracted from the stray light diffusion of the diamond anvils and optical parts. An evaluation of the compressibility of CsCdBr₃ was obtained by relative length measurements under a microscope by a direct photographic method, up to 5 GPa.^{12,13}

III. RAMAN SCATTERING: RESULTS AND ANALYSIS

A. General features of Raman spectra

Raman spectra from CsCdBr₃ have been reported^{16,17,20,21} at temperatures down to 4.2 K at ambient pressure. Standard factor-group analysis for this crystal predicts five Raman-active modes,

$$\Gamma = 1A_{1g} + 1E_{1g} + 3E_{2g}.$$

The three E_{2g} modes will be labeled with indices *a*, *b*, and *c* in order of increasing frequency throughout this paper. A study of the normal-mode eigenvectors has been made for other isomorphs:²² CsNiCl₃ and CsMgCl₃. They are shown in Fig. 2. For the discussion, the following remarks are in order.

(i) The motion of cadmium atoms does not give rise to any Raman mode.

(ii) The E_{2g}^a mode only involves Cs⁺ ion displacements in the *x-y* plane.

(iii) E_{1g} and E_{2g}^b involve bromine motions in the *z* and *x-y* directions, respectively. These two modes are strictly correlated in their physical origin: they correspond to the two components of motion of bromine due to the rotation of (CdBr₆)⁴⁻ octahedra around an axis in the *x-y* plane. In fact, they have been found to be nearly degenerate in frequency in some isomorphous compounds like CsNiCl₃ or CsMgCl₃,²²⁻²⁴ and this has on occasion made symmetry assignments difficult.




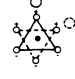
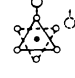
mode	wave number (cm ⁻¹)		
A_{1g}	161.5		symmetric breathing
E_{2g}^c	107		antisymmetric breathing
E_{2g}^b	75		chain libration ($\perp c$)
E_{1g}	55		chain libration ($\parallel c$)
E_{2g}^a	42		cesium vibration ($\perp c$)

FIG. 2. Eigenvectors for the five Raman-active modes viewed in the *c*-axis direction. Wave numbers are given for ambient conditions. No mode implies vibrations of the Cd²⁺ ion. Atoms drawn as in Fig. 1.

(iv) The two high-frequency modes E_{2g}^c and A_{1g} are the antisymmetric and symmetric breathing modes of the octahedra in the *x-y* plane. Typical spectra at different pressures are shown in Fig. 3. The number of Raman-active modes (5) is preserved over all the pressure range of our experiments: no splittings or new modes were observed. Mode E_{1g} is not detectable at the highest pressures, but this is due to a smooth and gradual decrease of its intensity by a factor of 10, which disguises it. It does not suddenly disappear, as might be the case at a change of symmetry (phase transition). For comparison, in the polytypic sequence relevant to this structure, 13 modes were observed^{20,24} in 6*H*-CsCdCl₃ (D_{6h}^4) and nine modes in 9*R*-CsMnCl₃ (D_{3d}^5). Thus Raman spectra under pressure at 300 K show no sign of any transition up to 25 GPa.

B. Frequency shifts

The pressure dependence of modes is shown in Fig. 4. We do not attempt here to draw an arbitrary curve through the data, for reasons which are discussed later on. In Fig. 4 the error boxes are different, from point to point, since they will depend on the intensity of the peaks, background intensity, pressure stability, etc. This represents spectra taken both at increasing and decreasing pressures since the measured frequencies were reproducible at a given pressure within experimental error, showing no measurable discontinuities or hysteresis at any point. This excludes first-order transitions with volume difference comparable (several percent) to those found in the polytypes obtained by application of high temperature and high pressure.

Nevertheless, other transitions might be present, such as second-order transformations or even weak first-order interpolytypic phase transitions which occur on occasion in low-dimensionality solids and may even preserve the space group of the crystal such as in the layered compound GaS.²⁵ These are usually accompanied by a

change in slope of the $\omega(P)$ curve, for one mode at least. Examination of Fig. 4 shows that the data could be accommodated with changes in the slope $\partial\omega/\partial P$ around 2, and possibly 10 GPa. Nevertheless closer analysis shows that even for E_{2g}^a , which shows the largest change in slope between low and high pressures, a second-degree polynomial fits the experimental data equally well. Figure 5 shows a series of experiments with a large number of experimental points in the low-pressure region which were an explicit search for second-order phase transition. This was negative: A quadratic fit with pressure reproduces the data better. It is shown for E_{2g}^a by comparison with straight-line fits with a change in slope at 2 GPa: Both are acceptable within experimental error and all modes can be fitted with a second-order polynomial, up to 10 GPa, or with a fourth-order polynomial which is slightly better, if we want to reproduce the $\omega(P)$ curves up to 25 GPa. This does not mean that no phase transition is present but that, on the basis of our experiments we cannot prove that they occur. In any case, the remarkable change in the slope of $\omega(P)$ is not conclusive evidence for phase transformations.

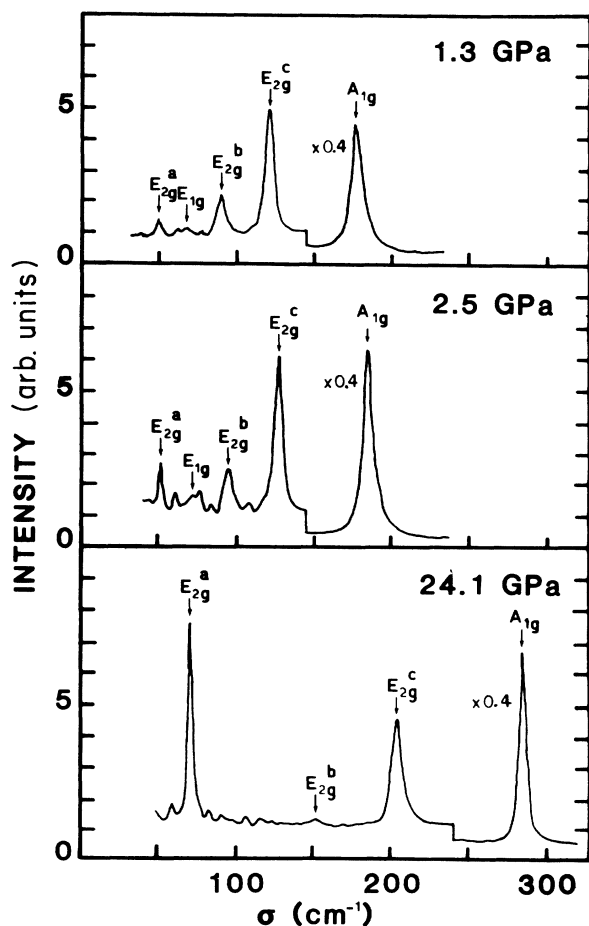


FIG. 3. Representative spectra at three different pressures. Spurious peaks in the region of 60–120 cm^{-1} , which are not identified by arrows, are due to emission from the optical system and do not vary with pressure. They have been identified by measuring the signal from the empty cell, and this background consistently subtracted from the total spectrum.

In Fig. 6 the behavior of $(1/\omega)(\partial\omega/\partial P)$ versus P has been fitted to the data by polynomial laws. The results for room pressure (linear term) are given in Table I. Examination of the results brings about the following conclusions.

(i) Except for E_{2g}^a , the linear pressure coefficients have an inverse correlation to frequency and their magnitude is comparable to that found in low-dimensionality (molecular) crystals:²⁶ in such structures, intramolecular modes (high frequencies) have pressure derivatives which are smaller than intermolecular ones (low frequencies) since the variation of the intermolecular space under pressure has a dominant contribution to the compression. Few chain crystals (1D) with chemical constituents analogous to those of CsCdBr₃ are known. We can compare with SbSI, or, better, SbSBr, which has been studied²⁷ in the same range of pressure. In these compounds, “interchain” modes, have eigenvectors similar to E_{1g} and E_{2g}^b , if one replaces two bromines in CsCdBr₃ by the sulfur atom in SbSBr. In the latter, the pressure coefficients of these low-frequency modes (B_{1g} and A_{1g}) have large pressure coefficients $(1/\omega)(\partial\omega/\partial P)$ of

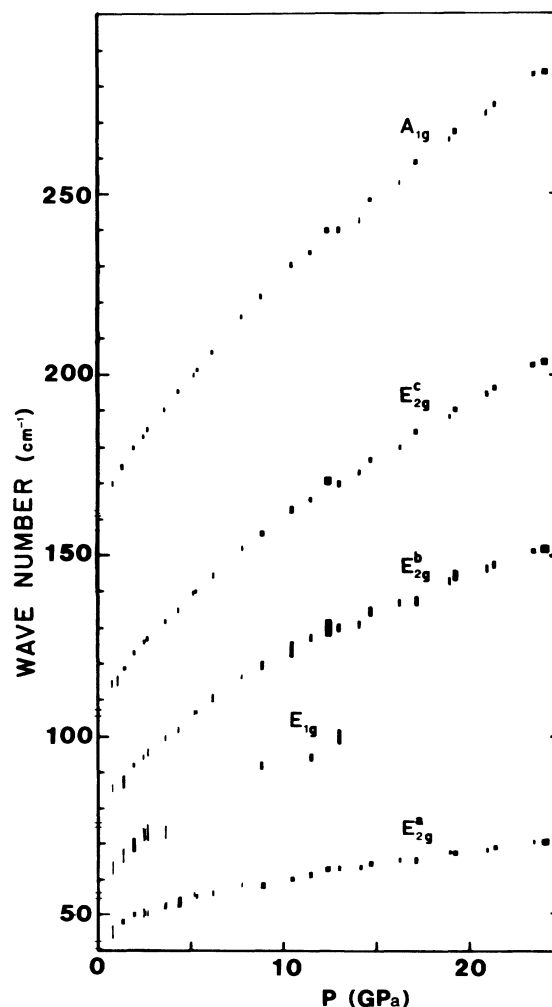


FIG. 4. Wave number of the modes versus pressure with argon as a pressure transmitting medium on increasing and decreasing pressure.

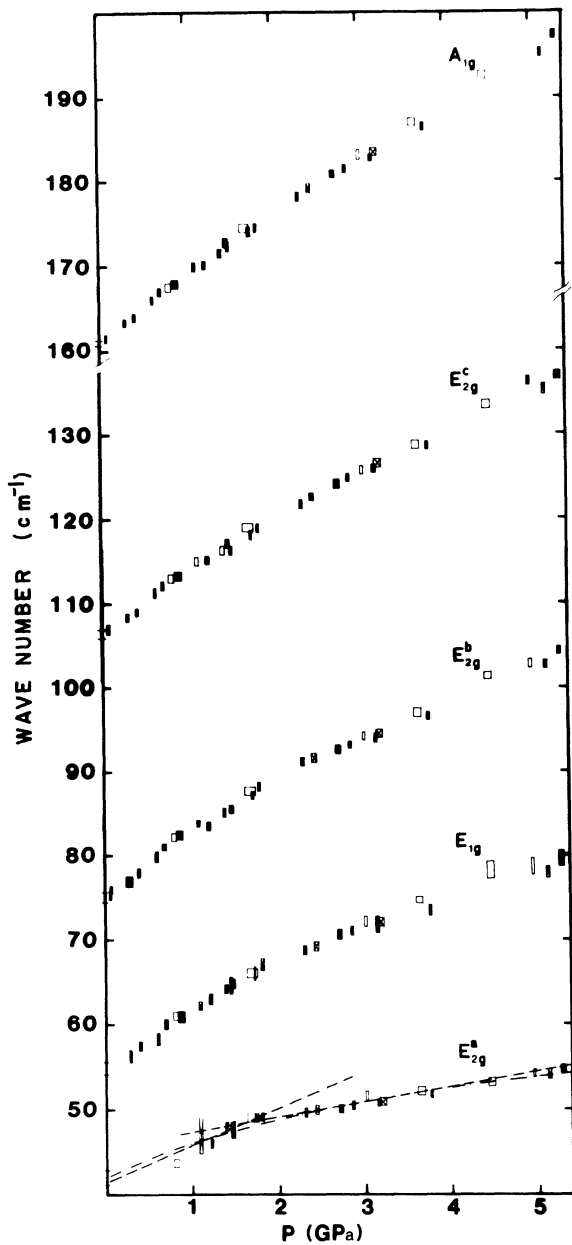


FIG. 5. Same as in Fig. 4 for two separate runs at lower pressure in silicone oil. Crosses, upstroke. Open rectangles, downstroke. Dashed line on mode E_{2g}^a is a best fit with two straight lines. Dash-dotted curve is a quadratic mean-square fit for comparison.

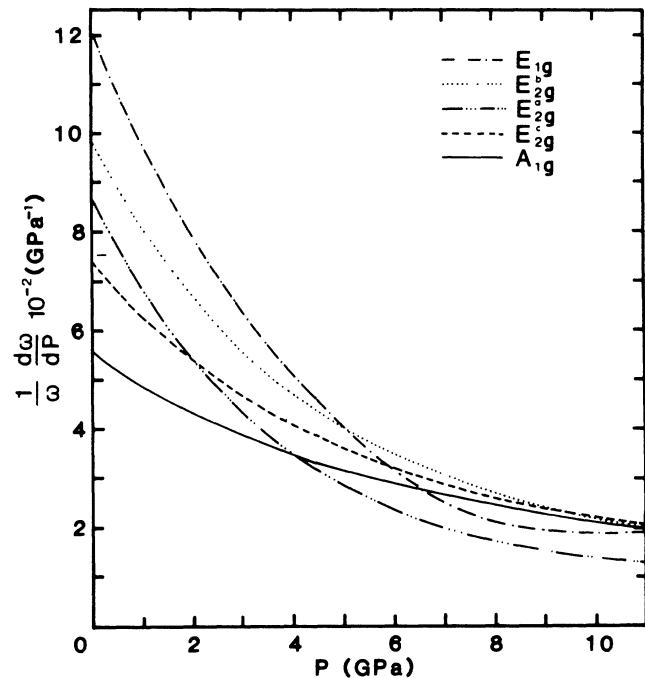


FIG. 6. Polynomial (fourth order) mean square fit of Figs. 4 and 5 for $(1/\omega)(d\omega/dP)$ vs P up to 10 GPa.

16×10^{-2} and 14×10^{-2} GPa^{-1} which compare well with 12×10^{-2} and 10×10^{-2} for E_{1g} and E_{2g} in CsCdBr_3 . Those large values are characteristic of low-dimensionality crystals.

(ii) Except again for E_{2g}^a , the pressure coefficients of the modes decrease with pressure and tend to a common value $\approx 2 \times 10^{-2}$ GPa^{-1} at high pressure (≈ 10 GPa), showing that restoring forces tend to be more and more similar at high pressure. This is also a general trend in low-dimensionality structures: interlayer and intralayer forces in layered crystals and interchain and intrachain forces in 1D crystals also tend to comparable magnitudes under high pressure.^{13,27}

(iii) In contrast, the E_{2g}^a mode which has the lowest frequency does not have the highest derivative with pressure. This is no surprise: this mode has no analog in bona fide molecular crystals where the space between molecular units (interchain space in SbSBr or SbSI) is empty. Another feature is its remarkable nonlinearity with pressure: at 10 GPa, its $(1/\omega)(\partial\omega/\partial P)$ is half

TABLE I. Relative pressure derivative of the modes: $(1/\omega)(d\omega/dP)$ at ambient pressure and temperature from the polynomial best fit discussed in text.

Mode symmetry	Frequency ω (cm^{-1})	Pressure coefficient at ambient $(1/\omega)(\partial\omega/\partial P)$ (10^{-2} GPa^{-1})
E_{2g}^a	42	9
E_{1g}	55	12
E_{2g}^b	75	10
E_{2g}^c	107	7.5
A_{1g}	161.5	5.5

(1×10^{-2} GPa⁻¹) that of the others as though the interchain space had become "harder," that is, less compressible than the chains themselves. Here again, this is not unexpected: even in molecular crystals where individual molecular units are linked by van der Waals forces, pressures of the order of 10 GPa will bring about such behavior. For instance, in GaS and GaSe, which are layered structures, compressibility and Raman scattering under pressure^{12,13} show that above some 10 GPa, the stiffness of the interlayer space becomes higher than in the intralayer space, no phase transition being involved.

Now in our case, the interchain space is occupied by xenonlike Cs⁺ ions which must be highly compressible at zero pressure but should tend with compression to a highly rigid hard-sphere behavior, as has been experimentally observed in recent studies of rare gases.²⁸ Xenon has a bulk modulus of 300 GPa at 30 GPa which makes it less compressible than, for instance, iron (190 GPa at ambient).

At low pressures, on the contrary, we expect the dodecahedral cages around Cs⁺ to be highly compressible as compared to the ionicovalent octahedral chains and to take the bulk of the volume variation under pressure. This is in keeping with a well-established model, the polyhedral representation of solids,²⁹ which has been widely used, notably by mineralogists, to understand the compression of metallic silicates, among others. The elementary polyhedra (SiO₄)²⁻ in the case of silicates are considered as rigid units, the compression being taken mostly by the "soft" metallic ions (Mg²⁺ or Fe²⁺ in olivines).

The same goes for perovskites, where the ionicovalent units are regular octahedra. In this case, the change in volume is accommodated by twisting the polyhedra which are linked by the summits or the edges.

Here (CdBr₆)⁴⁻ octahedra share a common face and no such twisting is possible. It seems, therefore, that the only choice would be a biaxial compression of the interchain space, which should lead to a large anisotropy in compressibility as is the case for SbSBr or SbSI, where the ratio of compressibilities perpendicular and parallel to the chains is about 100. This will be shown in Sec. V of this paper *not* to be the case and a coherent model of the evolution of forces in CsCdBr₃ will be drawn up after discussion of the rest of the experimental data.

C. Variation of Raman linewidths

In Fig. 7 are shown the full widths at half maximum of four modes with pressure. Too few reliable data have been obtained on the weak E_{1g} peak for it to be discussed. The only certain and clear trend observed concerns the totally symmetric A_{1g} stretching mode which decreases in width by a factor of 2 at 10 GPa. A study of A_{1g} in CsCdBr₃ at low temperature had already led us to propose that it was at ambient conditions, close to a Fermi-like resonance¹⁷ with a two-phonon density of states, possibly combinations of E_{1g} and E_{2g}^c branches away from the center of the Brillouin zone, which we suppose to be flat enough with increasing wave vector. We note that the sum of frequencies for those two

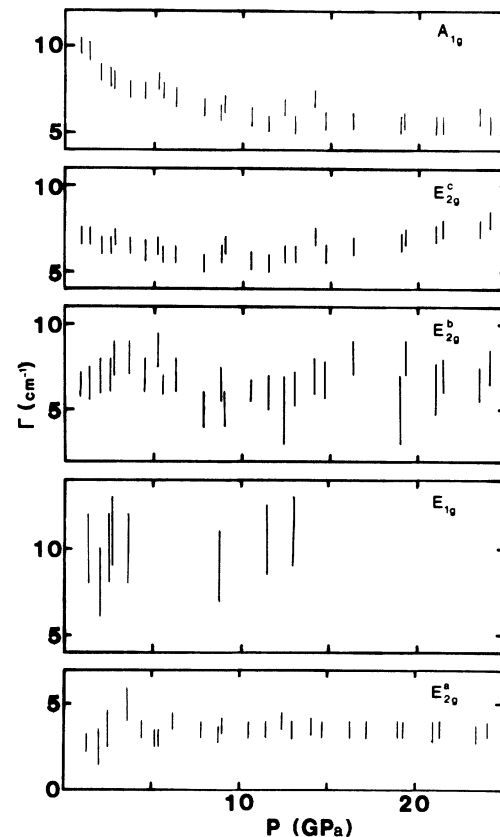


FIG. 7. Full widths at half maximum of individual Raman peaks. Γ , cm⁻¹. Error bars are largest for the weakest peaks.

center-of-the-zone modes is 162 cm⁻¹ at ambient as compared to 161.5 cm⁻¹ for A_{1g} . The pressure variation for this combination frequency will be about twice as large as that of A_{1g} and thus will move away from it in frequency when pressure is increased. Thus, above 10 GPa or so, we observe the unperturbed line shape of the totally symmetric mode. The difference between the A_{1g} mode frequency and the combination frequency of $E_{1g} + E_{2g}$ is taken as a gauge of the resonance strength and therefore of the damping of A_{1g} in Fig. 8. In this figure the in-

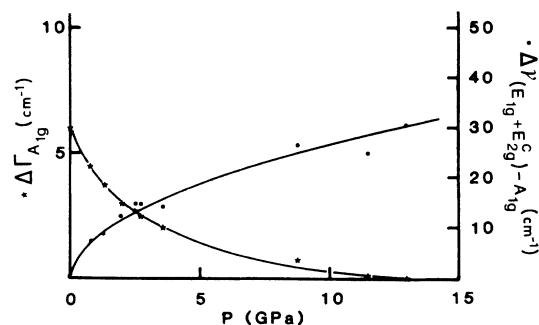


FIG. 8. Left-hand ordinates (stars), variation with pressure of the FWHM (Γ in Fig. 7) of A_{1g} . Γ has been taken as a constant above 15 GPa. Right-hand scale (solid circles), wave-number difference between the $E_{1g} + E_{2g}^c$ combination mode, and the A_{1g} mode with pressure (see text).

crease of the FWHM of this mode is plotted versus pressure, together with the energy difference of A_{1g} and $E_{1g} + E_{2g}$: the correlation is evident and indicates that, as in previous studies at low temperature,^{10,16} the large temperature dependence of the A_{1g} mode FWHM is indeed due to increasing overlap with the two-phonon density of states. A more precise analysis is not possible at the present time for lack of knowledge of phonon dispersion curves and their pressure coefficient.

Apart from this mode, the behavior of which can be explained by lattice dynamics arguments, no significant FWHM variations have been found, as could be expected if small splittings due to weak phase transitions were present (lowering of symmetry). Those splittings, even if smaller than the width of the peaks, would have shown as irregularities in the FWHM variation with pressure.

D. Variation of relative intensities

As noted in the experimental part, the relative intensity of the individual Raman lines was gauged as the ratio of the surface (height times width) of each line to the total of all five lines. Since the orientation of each sample was random in a plane perpendicular to the optical axis, we give here the pressure dependence of intensities for a single sample. Nevertheless we verified on other samples that the relative intensities were similar within 20%, under pressure: this is due to the fact that although the illumination (laser light) was polarized, the optical components before and after the sample acted like effective polarization scramblers. In any case we shall discuss here only large (1 to 10) intensity variations. These are shown in Fig. 9. The following remarks may be made.

(i) Modes A_{1g} and E_{2g}^c involve stretching of the co-

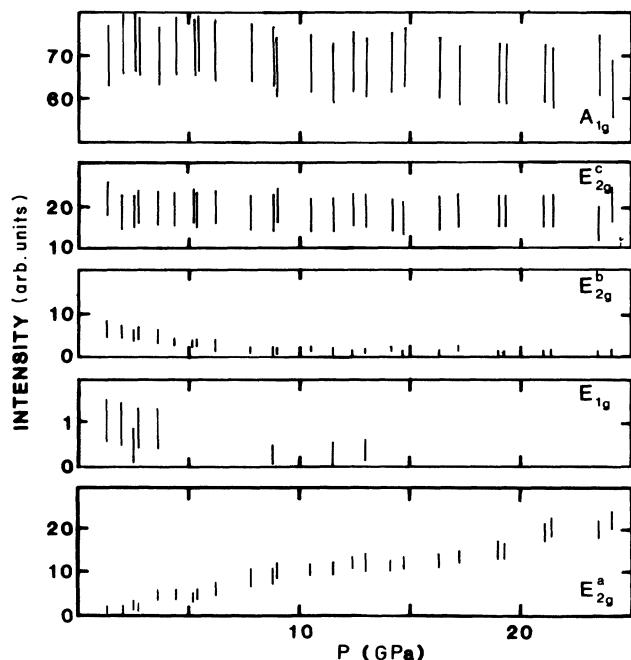


FIG. 9. Relative intensity of the modes in percent of total vs pressure (see text).

valent Cd—Br bond. Their intensity is constant with pressure, in keeping with the expected stability of this ionicovale bond, as regards the Cd—Br distance.

(ii) On the contrary, the E_{2g}^b mode decreases fast with pressure, roughly by 1 order of magnitude as well as its companion vibration E_{1g} , although for the latter the data are less precise. We note that the same behavior occurs in the corresponding modes in SbSBr, that is, for the low-frequency A_{1g} and B_{1g} modes which decrease strongly under pressure. In our case, CsCdBr₃, no unique explanation can be proposed for the decrease in Raman activity of the octahedra libration. We may only note that shear vibrations are not Raman active in the wholly symmetrical isolated octahedron. As will be seen in Sec. IV, this would be the consequence of application of high pressure, which should reduce the trigonal distortion of the octahedra along the c axis and contribute to reduction of the Raman activity of the modes through an increase in the local symmetry.

(iii) The E_{2g}^a mode (vibration of Cs⁺ in the x - y plane) shows a remarkable increase by a factor of 20 or so. This can be understood by examination of the Cs⁺ ion environment under pressure. At ambient, this ion is in a dodecahedron which we may for argument's sake take as bounded by the Br⁻ ions, leaving a quasispherical space about 2 Å in radius. Assuming the Br⁻ sites to have at most the radius of the free Br⁻ ion (1.96 Å at ambient pressure) this easily accommodates the Cs⁺ ion, the Pauling radius of which is only 1.60 Å. Its outer saturated electronic shell is thus in very weak interaction with its environment, even under the displacement along the E_{2g}^a phonon eigenvectors, which leaves unperturbed the high-symmetry electronic distribution.

The derivative of the dielectric function with respect to this type of displacement can be expected to be zero, which means no Raman activity. This is observed as a remarkably small Raman signal at room pressure.

Now under high pressure we expect the interchain Cs⁺ dodecahedra to take the bulk of the compression and thus to rapidly bring the outer electrons of Cs⁺ into contact with the walls of their dodecahedral cage. Then the E_{2g}^a phonon displacement will distort the electronic environment and charge transfer will occur, which will enhance the Raman activity. This point is semiquantitatively discussed thereafter.

IV. DISCUSSION

We noted previously the analogy of the high-pressure behavior of the chain modes frequency in CsCdBr₃ and 1D crystals like SbSBr. If this analogy were complete, we would expect to observe in crystals of the ABX_3 family a characteristic feature of molecular crystals which is the anisotropy of mechanical properties, the first and foremost being the compressibility tensor. In layered crystals the compressibilities perpendicular and parallel to the layers are in a ratio of 10, as an order of magnitude. The corresponding anisotropy in fibrous crystals, that is, the ratio of perpendicular to parallel to the chains, is of the order of 100.²⁷ This of course reflects the difference in magnitude between the intermolecular and

intramolecular forces in those structures.

The data on the compressibilities of ABX_3 compounds with the 2H structure are scarce. From ultrasonic measurements³⁰ in CsNiCl₃, one can derive the compressibility anisotropy which is only 1.8. Our own measurements, performed in the diamond anvil cell by the method described in Sec. I, give low-pressure (1 GPa) compressibilities: $\chi_{\parallel}=(2.5\pm 0.3)\times 10^{-2}$ GPa⁻¹ and $\chi_{\perp}=(2\pm 0.3)\times 10^{-2}$ GPa⁻¹ in directions parallel and perpendicular to the c axis. This volume variation is strongly nonlinear with pressure. The admittedly poor precision of our measurements is nonetheless sufficient for our discussion: in CsCdBr₃, as well as in CsNiCl₃, the elastic constant anisotropy is small and comparable to that currently found in three-dimensional solids. It is 1 order of magnitude smaller than in van der Waals layer crystals and two orders of magnitude smaller than that of 1D crystals²⁷ like SbSBr where $\chi_{\perp}=2.5\times 10^{-2}$ GPa⁻¹ and $\chi_{\parallel}=4.5\times 10^{-4}$ GPa⁻¹. So although the bulk compressibility $-1/V_0(\partial V/\partial P)$ of CsCdBr₃ ($\approx 6.5\times 10^{-2}$ GPa⁻¹) is comparable to that of SbSBr ($\approx 5\times 10^{-2}$ GPa⁻¹), its anisotropy is completely different.

It might be argued at this point that CdCsBr₃ at ambient could be compared with a 1D structure under high hydrostatic pressure, 10 GPa or so, because of the inner overpressure caused by ionic bonding. This also is misleading: the pressure coefficients of the phonon frequencies at high pressure in SbSBr are 1 order of magnitude smaller than those of CsCdBr₃ at ambient because of their nonlinear behavior.

To sum up the points which have been discussed in this paper, based on our work and previous studies, we have to find a coherent model for CsCdBr₃ which will reconcile the following.

- (i) The short-range anisotropy of bonds at ambient is proven by its magnetic and energy transfer properties.
- (ii) Covalent octahedra must be much less compressible than the rhombododecahedral cages of the Cs⁺ ions, as is the case in a large number of crystals (minerals among others), where the polyhedral approach has been successfully applied.
- (iii) The pressure dependence of the covalent chain modes is comparable to that of SbSBr.
- (iv) Volume compressibilities are similar in both, but the compressibility anisotropy is not: CsCdBr₃ behaves like a soft isotropic molecular crystal in that respect.

To explain these trends, we propose a qualitative model based on the nature of the bonds.

At ambient pressure, let us view first CsCdBr₃ as an assembly of strings of covalent octahedra separated by chains of Cs⁺ in a rhombododecahedral environment. The former are negatively charged and the latter positively. Thus the Coulomb interaction will tightly pack this assembly, bringing the fibers close together in the x - y plane. The overpressure will thus be highly anisotropic, with a strong biaxial component, which is equivalent to a hydrostatic (isotropic component) plus a negative component along the z axis (tension). This accounts for the initial elongation of the covalent chains along z , and consequent decrease of the angle between the Br—Cd bonds and the c axis. Now if the bundle of such chains is bound

tight enough by the Coulomb glue, we do not expect as strong an anisotropy in the compressibility tensor as in 1D structures where the fibers are, on the contrary, very loosely bound. This accounts for point (iv).

Under pressure, the anisotropic ionic contribution should as a whole be less and less important with respect to pressure-induced interactions. This is expected in general and has recently been well verified, for instance, in CsI, which is isoelectronic with xenon: at high pressures, the ionic interactions become negligible with respect to those brought about by outer shell overlap and indeed the equation of state²⁸ of both are almost identical above 10 GPa. Qualitatively at least we expect the same here: the ionic contribution to interatomic restoring forces relative to other interactions brought about by pressure will decrease and thus the initial elongation of the (CdBr₆)⁴⁻ octahedra should decrease, their volume remaining constant (or decreasing less than the rest of the crystal). The octahedra will tend to be more regular by opening the (CdBr₃)⁻ trihedra along the c axis. This accounts for the component of compressibility along the c axis. A consequence is an increase of the fraction of the space occupied by covalent chains in the x - y directions. This has to be accommodated by a stronger elongation of the Cs⁺ dodecahedral cages along c . CdBr₆ units thus tend to be closer to regular octahedra and the increase in local symmetry might cause the decrease of the intensity of E_{1g} and E_{2g}^b .

In this model, the relative volume occupied by the Cs⁺ ions has to decrease faster than that of the covalent chains. This is necessary to account for the increase of the Raman cross section of the E_{2g}^a mode and the behavior of the pressure derivative $(1/\omega)(\partial\omega/\partial P)$ of this mode (Fig. 6), which becomes smaller than that of the other modes above 4 GPa or so. To evaluate this effect semi-quantitatively, we shall proceed along the following lines: the total volume of the crystal is made up of the space occupied by the ionicovalent (CdBr₃)⁻ units, plus the cesium ions rhombododecahedra, limited by planes tangent to the 12 nearest bromine ions. To simplify, we neglect the trigonal distortion and approximate the ellipsoidal Cs⁺ environment by spheres. The total decrease in volume of the crystal is known from our optical compressibility measurements. We then compute the compression of the ionicovalent chains alone from the general bulk modulus-volume relationships which have been established for cation-anion polyhedra.²⁹ The rest of the compression has to be taken up by the quasispherical environment of cesium, which gives us an evaluation of the variation in volume of the Cs⁺ ion effective radius under pressure. We do this calculation at 4 GPa since, as noted above, the behavior of the E_{2g}^a mode changes in this pressure range.

A. Bulk compression of the crystal

We will from now on operate for simplicity on the volume V of half a unit cell (one CsCdBr₃ formula unit) which is $V_0=172$ Å³ at ambient.⁸ The compressibility decreases markedly with pressure from its room pressure value of 6.5×10^{-2} GPa⁻¹ and our measurements show a

total volume decrease of only 15% at 4 GPa, which gives

$$V = 0.85V_0 = 146 \text{ \AA}^3.$$

B. Volume variation of the ionicovalent chains

To compute this we first have to determine their volume fraction relative to the total of the crystal at ambient by subtracting the volume occupied by cesium ions. At zero pressure, the Cs-Br distance⁸ is 3.93 Å, averaging over the distances. We do not know the proportion of ionic and covalent bondings in the $(\text{CdBr}_3)^-$ subunits so, for want of better knowledge, we take the Br^- ion radius to be 1.96 Å (or less) and thus the Cs^+ sphere should be $3.93 - 1.96 = 1.97$ Å (or more). This compares well with published values¹⁵ of Cs^+ with a coordination number of 12, which is 2.02 Å. We take $r = 2$ Å to be close enough and this gives a volume of $(4\pi/3)r^3 = 33 \text{ \AA}^3$ for the cesium cages. This leaves out $172 - 33 = 139 \text{ \AA}^3$ for the CdBr_3 units, at ambient.

We now turn to Ref. 29 to evaluate the local compression of those units, where cadmium is at most Cd^{2+} and bromine Br^{1-} . We can use either the bulk modulus relationship for halides which is

$$K_p \langle d \rangle^3 / Z_c = 560 \text{ GPa \AA}^3 \quad (2)$$

or the general relation for cation-anion polyhedra,

$$K_p \langle d \rangle^3 / S^2 Z_c Z_a = 750 \text{ GPa \AA}^3, \quad (3)$$

with K_p the polyhedral bulk modulus (GPa), $\langle d \rangle$ the mean cation-anion separation (Å), Z_c and Z_a the cation and anion formal charges, respectively, and S^2 an empirical term giving the relative ionicity of the bonds.

In our case, $d = 2.77$ Å, $Z_c = 2$, $Z_a = 1$, and $S^2 = 0.75$, as in metal halides.²⁹ Either formula gives $K_p \approx 50$ GPa, which corresponds to a decrease of 8% in volume at 4 GPa. This brings the volume of CdBr_3 units down to

$$139 \times 0.92 = 128 \text{ \AA}^3.$$

C. Variation of the volume occupied by the Cs^+ ion

At ambient, this volume was $\approx 33 \text{ \AA}^3$. At 4 GPa it is the difference between the total volume of a half unit cell (146 \AA^3) and that of the CdBr_3 subunit (128 \AA^3), that is, 18 \AA^3 . This corresponds to a radius of ≈ 1.6 Å for the

Cs^+ ion. This is comparable to the Goldschmidt (1.65 Å) or Pauling (1.60 Å) radii for cesium, and much smaller than the room-pressure (≈ 2 Å) radius.

This evaluation is admittedly rough, but even with generous allowance for errors on K_p and our compressibility data (20%) one still finds the Cs^+ radius to decrease from 2 Å down to ≈ 1.6 Å between 3 and 5 GPa, which is sufficient precision to make our point. Above this pressure range, the stiff xenonlike filled electronic shell around the ion starts overlapping with bromine orbitals and gradually tends to rigid sphere behavior: The local environment of Cs^+ , which was softer than the rest of the crystal, at ambient, becomes harder (less compressible) at high pressure.

This accounts for the noticeable change in slope for $(1/\omega)(\partial\omega/\partial P)$ of the E_{2g}^a mode, the changeover between the soft ionic regime, and the hard-sphere filled shell regime being in the vicinity of 4 GPa.

CONCLUSION

The variation under pressure of this type of structure can thus be qualitatively understood in terms of the anisotropy of the bonding scheme. Although this structural anisotropy is reflected in short-range phenomena like magnetic ordering or Raman vibrations, it does not bring about long-range anisotropy in compressibility or elastic constants as observed in van der Waals bonded, low-dimensionality crystals. This is due to the Coulomb interaction of negatively charged ionicovalent chains separated by positively charged alkali ion chains. Although the semiquantitative model that we used here is admittedly naive and oversimplified, it gives the right order of magnitude for the pressure (≈ 4 GPa) where the Cs^+ space changes over from van der Waals-ionic regime, to hard-sphere behavior, as shown by the evolution of the Raman tensor of the E_{2g}^a mode, and the change in the pressure derivative of this mode.

ACKNOWLEDGMENTS

Physique des Milieux Condensés is "Unité Associée au Centre National de la Recherche Scientifique No. 782." Laboratoire de Physico-chimie des Matériaux is "Équipe de Recherche No. 211." Università degli Studi di Trento is Centro Interuniversitario di Struttura della Materia, Ministero della Pubblica Istruzione.

¹O. Muller and R. Roy, in *The Major Ternary Structural Families*, edited by R. Roy (Springer-Verlag, Berlin, 1976).

²J. M. Longo and J. A. Kafalas, *Mater. Res. Bull.* **3**, 687 (1968).

³J. M. Longo and J. A. Kafalas, *J. Solid State Chem.* **1**, 103 (1969).

⁴Y. Syono, S. Akimoto and K. Kohn, *J. Phys. Soc. Jpn.* **26**, 993 (1969).

⁵W. B. Euler, L. E. Mohrmann, Jr., and B. B. Garrett, *J. Magn. Reson.* **35**, 185 (1979).

⁶N. Achiwa, *J. Phys. Soc. Jpn.* **27**, 561 (1969).

⁷Y. Syono, S. Akimoto, and K. Kohn, *J. Phys. Soc. Jpn.* **26**, 993 (1969).

⁸G. L. McPherson, A. M. McPherson, and J. L. Atwood, *J. Phys. Chem. Solids* **41**, 495 (1980).

⁹G. L. McPherson, M. H. Nodine, and K. O. Devaney, *Phys. Rev. B* **18**, 6011 (1978).

¹⁰C. Andraud, Thèse d'Etat, Université Pierre et Marie Curie, Paris, 1987.

¹¹C. Andraud, F. Pellé, O. Pilla, J. P. Denis, and B. Blanzat, *J. Phys. (Paris), Colloq.* **46**, C7-489 (1985).

- ¹²M. Gauthier, A. Polian, and J. M. Besson, *J. Phys. (Paris), Colloq.* **45**, C8-65 (1984).
- ¹³A. Polian, J. C. Chervin, and J. M. Besson, *Phys. Rev. B* **22**, 3049 (1980).
- ¹⁴A. Polian, J. M. Besson, M. Grimsditch, and H. Vogt, *Phys. Rev. B* **25**, 2767 (1982).
- ¹⁵R. D. Shannon and G. I. Prewitt, *Acta Crystallogr. Sect. B* **25**, 925 (1969).
- ¹⁶O. Pilla, E. Cazzanelli, C. Andraud, B. Blanzat, and F. Pellé, *Cryst. Latt. Def. Amorphous Mat.* **16**, 301 (1987).
- ¹⁷O. Pilla, E. Cazzanelli, C. Andraud, B. Blanzat, and F. Pellé, *Physica Status Solidi B* **144**, 845 (1987).
- ¹⁸C. E. Weir, C. J. Piermarini, and S. Block, *Rev. Sci. Instrum.* **40**, 1133 (1969).
- ¹⁹H. K. Mao, P. M. Bell, J. W. Shaner, and D. J. Steinberg, *J. Appl. Phys.* **49**, 3276 (1978).
- ²⁰C. W. Tomblin, G. W. Jones, and R. W. G. Syme, *J. Phys. C* **17**, 4345 (1984).
- ²¹A. V. Orinchai, V. B. Lazarev, E. Yu Peresh, B. M. Koperlos, and V. S. D'ordyay, *Izv. Akadem. Nauk. SSSR, Neorg. Mater.* **18**, 1281 (1982) [*Inorg. Mater. (USSR)* **18**, 1080 (1982)].
- ²²I. Nakagawa and Y. Morioka, in *Spectra and Dynamics of Ionic Crystals*, Vol. 9 of *Vibrational Spectra and Structure*, edited by J. Durig (Elsevier, Amsterdam, 1981), p. 75.
- ²³M. H. Brooker and Chung-Hsi Huang, *Mater. Res. Bull.* **15**, 9 (1980).
- ²⁴I. W. Johnstone, G. D. Jones, and D. J. Lockwood, *Solid State Commun.* **39**, 395 (1981).
- ²⁵I. Rannou, Ph.D. Thesis, Université Paris VI, 1986.
- ²⁶R. Zallen, *Phys. Rev. B* **9**, 4485 (1974); R. Zallen and M. L. Slade, *ibid.* **18**, 5775 (1978).
- ²⁷J. F. Vittori, Ph.D. thesis, Université Paris VI, 1982; J. F. Vittori, M. Teng, S. Ziolkewicz, and A. Polian (unpublished).
- ²⁸A. N. Zisman, A. V. Aleksandrov, and S. M. Stishov, *Pis'ma Zh. Eksp. Teor. Fiz.* **40**, 253 (1984) [*JETP—Lett.* **40**, 1029 (1984)].
- ²⁹R. M. Hazen and L. W. Finger, *J. Geophys. Res.* **84**, 6723 (1979). A review of the polyhedral method and structural variations of solids under pressure may be found in R. M. Hazen and L. W. Finger, *Comparative Crystal Chemistry* (Wiley, New York, 1982), and references therein.
- ³⁰K. R. Mountfield and J. A. Rayne, *J. Phys. (Paris), Colloq.* **42**, C6-468 (1981).